Hindawi
Scientific Programming
Volume 2021, Article ID 4258360, 8 pages
https://doi.org/10.1155/2021/4258360

Research Article

Backpropagation Neural Network Algorithm-Based Color Doppler Ultrasound Detection of Gestational Diabetes Mellitus and Perinatal Outcomes

Xiaoqing Zhang, Yinsu Lou, Sunhao Hu, and Dan Zhu

Department of Obstetrics, Yiwu Central Hospital, Yiwu 322000, Zhejiang, China

Correspondence should be addressed to Xiaoqing Zhang; 20200120877@nxmu.edu.cn

Received 5 June 2021; Accepted 12 July 2021; Published 20 July 2021

Academic Editor: Gustavo Ramirez

In this work, the related risk factors and perinatal outcomes of pregnant women with gestational diabetes mellitus (GDM) were analyzed based on color Doppler ultrasound (CDU) diagnosis. Backpropagation (BP) algorithm-based CDU imaging algorithm (BPC) was constructed in this study and applied in CDU images of 80 pregnant women with GDM. Besides, amplitude and phase estimation (APES) and low-complexity adaptive beam (LCA) algorithms were introduced for comparison with BPC in turn. It was found that Dice similarity coefficient (96.44%), sensitivity (95.45%), and specificity (91.56%) of BPC were greater than those of APES (83.97%, 85.84%, 78.45%) and LCA (84.74%, 86.29%, 82.35%), while its running time (6.44 ± 1.39 s) was shorter than that of APES (11.87 ± 2.41 s) and LCA (13.76 ± 1.54 s) ($P < 0.05$). Pregnant women in the experimental group (group B) were older than those in the control group (group A) ($P < 0.05$). The pulsatility index (PI) and renal artery resistance index (RI) of fetuses in group B (0.95 ± 0.15) were higher than those of group A (0.57 ± 0.24) ($P < 0.05$). In addition, pregnancy age, family history of hypertension, and abortion history were positively correlated with GDM ($P < 0.05$). In conclusion, BPC could not only improve diagnosis accuracy in fetuses' CDU images but also shorten calculation time. Pregnancy age, family history of hypertension, and abortion history were the related risk factors for GDM in pregnant women.

1. Introduction

DM is a metabolic disease caused by a variety of pathogenic factors, which is mainly manifested as chronic hyperglycemia and characteristic of multisystem dysfunction caused by carbohydrate, fat, and protein metabolism [1]. What is more, GDM is a type of DM which only appears or is diagnosed during pregnancy [2]; that is, the patient has glucose metabolism before pregnancy. The incidence of GDM is about 1%–14% worldwide while it is about 1%–5% in China. The GDM patients in China account for about 80% of pregnant women with DM, which has increased in recent years [3]. The GDM will weaken the heart function of the fetus and cause hypoxia or even asphyxia in the fetuses [4]. The clinical treatment process of GDM is very complicated, which puts both the mother and the fetus at risk. Therefore, the exploration of risk factors for GDM is beneficial to reducing the incidence of perinatal complications [5].

CDU, also known as B-ultrasound and color ultrasound, is suitable for the ultrasound examination of various parts of the body, especially for the examination and diagnosis of the heart, limb blood vessels, superficial organs, abdomen, obstetrics, and gynecology. It is a noninvasive technology to examine the intracardial shunt and reflux [6, 7], which involves autocorrelation technology for Doppler signal processing. The blood flow signal obtained by autocorrelation technology is color-coded and superimposed on a two-dimensional image in real time. It not only has the advantages of two-dimensional ultrasound images but also provides rich information on hemodynamics [8, 9]. Deep learning is a branch of machine learning. Besides, deep

learning is an algorithm for characterizing and learning data, which adopts artificial neural networks (ANN) as the framework, mainly including deep neural networks, convolutional neural networks, deep belief networks, and recurrent neural networks [10]. BP is a common method applied in combination with optimization methods (such as gradient descent method) to train ANN and is adopted to calculate the gradient of the loss function for all weights in the network, which will be fed back to update the weights to minimize the loss function for the optimization of the color Doppler image [11, 12]. Therefore, the BP neural network algorithm was adopted in this study to analyze the CDU images of patients.

To sum up, deep learning technology has a wide range of applications in clinical imaging diagnosis. Based on this, APES and LCA were introduced for comparison with the established BPC in turn, and BPC was used for CDU imaging diagnosis of 80 cases with GDM, so as to comprehensively evaluate the related risk factors and perinatal outcomes of pregnant women with GDM.

2. Materials and Methods

2.1. Selection of Research Samples. 80 pregnant women diagnosed pathologically as having GDM were selected in group B in this study, who were treated in the hospital from May 18, 2018, to October 20, 2019. Besides, 80 healthy pregnant women were in group A. The experiment had been approved by the Medical Ethics Committee of the hospital, and each patient and his/her family members had understood the situation of this experiment and signed the informed consent forms.

The inclusion criteria are as follows: patients who were diagnosed as GDM pathologically; the primipara; patients who did not take drugs that interfered with glucose and fat metabolism; patients younger than 45 years old; and patients with clear consciousness.

The exclusion criteria are as follows: patients who had a mental illness; patients suffering from other diseases such as hypertension, kidney, and cardiovascular; patients who smoked or drank alcohol; and patients who withdrew from this experiment due to personal reasons.

2.2. Diagnostic Standards for Gestational Diabetes Mellitus. The diagnostic standards in this study were according to the sixth edition of *Obstetrics and Gynecology (People's Medical Publication House)*. First, group B were screened with 50 g of glucose at the 25^{th}–28^{th} weeks. If the blood glucose level was higher than 7.9 mmol/L after 1 hour, the patient was confirmed to be positive of glucose screening and then examined for fasting blood glucose. If the blood glucose level was abnormal, the patient was diagnosed as having GDM. The healthy pregnant women underwent an oral glucose tolerance test (OGTT). Further, 75 g OGTT was performed, with 5.6 mmol/L being the fasting blood glucose content upper limit under normal conditions. The blood glucose content 1 hour, 2 hours, and 3 hours after a meal was 10.3 mmol/L, 8.6 mmol/L, and 6.7 mmol/L, respectively. If the content of two or more terms exceeded the normal range, the patient was diagnosed as GDM.

2.3. Doppler Ultrasound Examination Method. GEV730 and Philips U22 color Doppler ultrasound diagnostic apparatuses were adopted in this study, and the frequency of the probe was 3.5–5.0 MHz. The pregnant woman took the supine position and was asked about the results of the ultrasound diagnosis in the early pregnancy and the time of the last menstruation. After the pregnancy cycle was determined, the routine growth indexes of obstetrics were measured, including the head circumference, biparietal diameter, femur, and abdominal circumference of every fetus. The ultrasonic probe was placed at the junction of the umbilical artery and the placenta. During the detection process, a closer distance between the probe and the placenta indicates a more accurate measurement value. The angle between the Doppler sampling line and the blood vessel should be less than 25°, the blood flow velocity of the umbilical artery should be recorded accurately, and the spectrogram should be preserved during this experiment. Moreover, the cross-sectional image of the fetal brain was obtained based on the double parietal diameter, and the Doppler ultrasound signals were acquired on the side close to the middle cerebral artery. RI, PI, ventricular systolic peak velocity (S), ventricular diastolic peak velocity (D), and atrial systolic maximum velocity (A) should be recorded, and the S/D value was calculated.

2.4. Parallel Beam Filtered Backprojection Algorithm. The two-dimensional Fourier inverse transform was employed, so as to obtain the original image $g(x, y)$, expressed as the following equation:

$$g(x, y) = \int_{-\infty}^{\infty} \int_{-\infty}^{\infty} G(a, b)^{ej2\pi(ax+by)} \mathrm{d}a\mathrm{d}b. \tag{1}$$

Polar coordinate (α, β) was converted from a rectangular coordinate system (a, b), expressed as follows:

$$\begin{aligned} a &= \alpha \cos \beta, \\ b &= \alpha \sin \beta. \end{aligned} \tag{2}$$

In equation (2), a and b are the horizontal and vertical coordinates, respectively, and α and β are the angular dimensions. The partial derivative of a and b is expressed as

$$\mathrm{d}a\mathrm{d}b = \begin{vmatrix} \dfrac{\partial a}{\partial \alpha} & \dfrac{\partial a}{\partial \beta} \\ \dfrac{\partial b}{\partial \alpha} & \dfrac{\partial b}{\partial \beta} \end{vmatrix} \mathrm{d}\alpha\mathrm{d}\beta = \alpha \mathrm{d}\alpha\mathrm{d}\beta, \tag{3}$$

where $\mathrm{d}a\mathrm{d}b$ is the partial derivative of a, b. Equations (2) and (3) are substituted into equation (1), to get the following equation:

$$g(x,y)=\int_0^{2\pi}\mathrm{d}\beta\int_0^{\infty}G(\alpha\cos\beta,\alpha\sin\beta)e^{j2\pi(x\cos\beta+y\sin\beta)}\alpha\mathrm{d}\alpha. \tag{4}$$

According to the Fourier slice theorem, $G(\alpha\cos\beta,\alpha\sin\beta)$ is replaced by $Q(\alpha,\beta)$ to obtain the following:

$$g(x,y)=\int_0^{2\pi}\mathrm{d}\beta\int_0^{\infty}G(\alpha,\beta)e^{j2\pi\alpha(x\cos\beta+y\sin\beta)}\alpha\mathrm{d}\alpha. \tag{5}$$

The projection process is symmetric. Besides, a set of rays differ by 180°, and the two paths coincide. Thus, the following equation is obtained:

$$Q(s,\beta+\pi)=Q(-s,\beta), \tag{6}$$

where s is the angular dimension. Due to the special properties of the Fourier transform, there is a corresponding Fourier transform equation as follows:

$$Q(\alpha,\beta+\pi)=Q(-\alpha,\beta). \tag{7}$$

Equation (7) is then substituted into equation (5) to obtain the following equation:

$$g(x,y)=\int_0^{\pi}\mathrm{d}\beta\int_{-\infty}^{\infty}Q(\alpha,\beta)|\alpha|e^{j2\pi\alpha(x\cos\beta+y\sin\beta)}\mathrm{d}\alpha. \tag{8}$$

In equation (8), $Q(\alpha,\beta)$ is the Fourier transform of the projection at the angle α. It is multiplied by $|\alpha|$ after the Fourier transform is completed. In the space domain, the projection is made by filtering function of frequency domain $|\alpha|$, called the filtered back projection. If $h(s,\beta)$ is filtered backprojection, equation (9) is obtained as follows:

$$h(s,\beta)=\int_{-\infty}^{\infty}Q(\alpha,\beta)|\alpha|e^{j2\pi\alpha(x\cos\beta+y\sin\beta)}\mathrm{d}\alpha. \tag{9}$$

Then, the following equation is obtained based on equation (8):

$$g(x,y)=\int_0^{\pi}h(s,\beta)\mathrm{d}\beta=\int_0^{\pi}h(x\cos\beta+y\sin\beta)\mathrm{d}\beta. \tag{10}$$

Equation (10) indicates that all filtered projections passing through $g(x,y)$ should be accumulated if the value of $g(x,y)$ at a certain position in the area needs to be reconstructed. Then, a suitable spatial domain function $f(s)$ is selected for the Fourier transform, and the function $f(s)$ is backpropagated to the projection:

$$g(x,y)=\int_0^{\pi}\mathrm{d}\beta\int_{-\infty}^{\infty}Q(s',\beta)f(s-s')\mathrm{d}s', \tag{11}$$

where s' is the postprojection parameter of s. The above is the CDU imaging algorithm constructed in this study based on the BP neural network, which is abbreviated as BPC.

2.5. Algorithm Performance Evaluation Indexes. APES [13] and LCA [14] were introduced for comparison with the constructed BPC. The Dice similarity coefficient, sensitivity, specificity, and running time were selected as the evaluation indexes of algorithm performance, which were calculated as follows:

$$\mathrm{Dice}=2\times\frac{|T_1\cap T_2|}{|T_1|+|T_2|}, \tag{12}$$

$$\mathrm{Se}=\frac{\mathrm{TP}}{\mathrm{TP}+\mathrm{FN}}\times100\%, \tag{13}$$

$$\mathrm{Sp}=\frac{\mathrm{TN}}{\mathrm{TN}+\mathrm{FP}}\times100\%. \tag{14}$$

In equations (12)–(14), T_1 is the professional evaluation result; T_2 is the diagnostic result of the algorithm; and TP, TN, FP, and FN represent true positive, true negative, false positive, and false negative, respectively.

2.6. Statistical Methods. The data was processed by SPSS19.0, the measurement data was expressed as the mean ± standard deviation ($\overline{x}\pm s$), and the count data was represented by the percentage (%). The t-test was for comparison between APES, LCA, and BPC in Dice similarity coefficient, sensitivity, specificity, and running time. The analysis of variance was comparison in the pregnancy age, exercise history, breakfast history, body mass index (BMI), pulmonary vein indexes (S, D, S/D, A, and Tei index), PI and RI of pregnant women, and gestational age and birth weight of fetuses. A multiple regression model was adopted to analyze the risk factors of GDM in pregnant women. $P<0.05$ was set as the threshold for significance.

3. Results

3.1. Comparison of the Diagnostic Performance of the Three Algorithms. Figures 1 and 2 show the comparison results of the Dice similarity coefficient, sensitivity, specificity, and running time of the three algorithms. It was found that the Dice similarity coefficient of APES was 83.97%, its Se was 85.84%, its Sp was 78.45%, and its running time was 11.87 ± 2.41 seconds. The Dice similarity coefficient, Se, Sp, and running time of LCA were 84.74%, 86.29%, 82.35%, and 13.76 ± 1.54 seconds in turn. Furthermore, the Dice of BPC was 96.44%, the Se was 95.45%, the Sp was 91.56%, and the running time was 6.44 ± 1.39 seconds. The results indicated that the Dice similarity coefficient, sensitivity, and specificity of BPC were hugely greater than those of APES and LCA, and the difference was statistically obvious ($P<0.05$). The running time of BPC was dramatically shorter than that of APES and LCA, and there was a statistically great difference ($P<0.05$).

3.2. Comparison of Basic Data of Pregnant Women in the Two Groups. Figure 3 shows the comparison results of pregnancy age, exercise history, and breakfast history (whether the subject had routine breakfast) of pregnant women in groups A and B. It could be seen that the pregnancy age of pregnant women in group B was obviously greater than that of group A, suggesting that the difference was statistically obvious ($P<0.05$). The number of pregnant

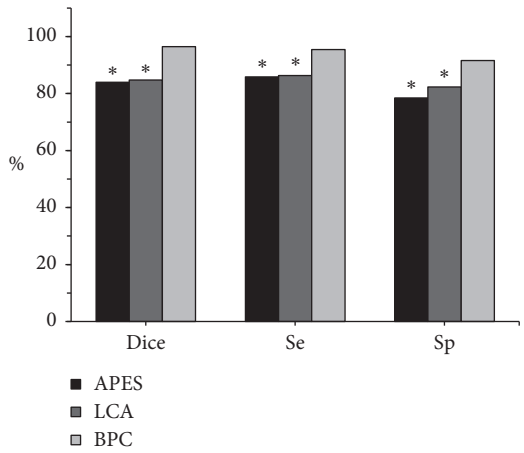

Figure 1: Comparison of the Dice similarity coefficient, sensitivity, and specificity of the three algorithms. *Note*. * expresses that the difference was statistically substantial in contrast to BPC, $P < 0.05$.

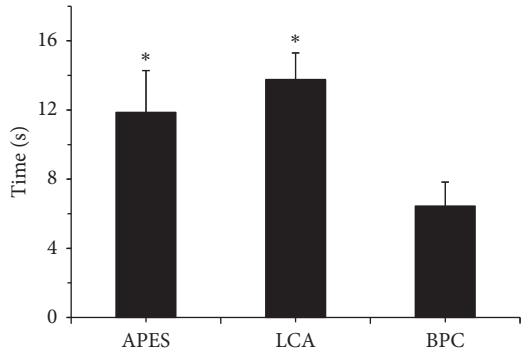

Figure 2: Comparison of the running time of the three algorithms. *Note*. * means that the difference was statistically substantial in contrast to BPC, $P < 0.05$.

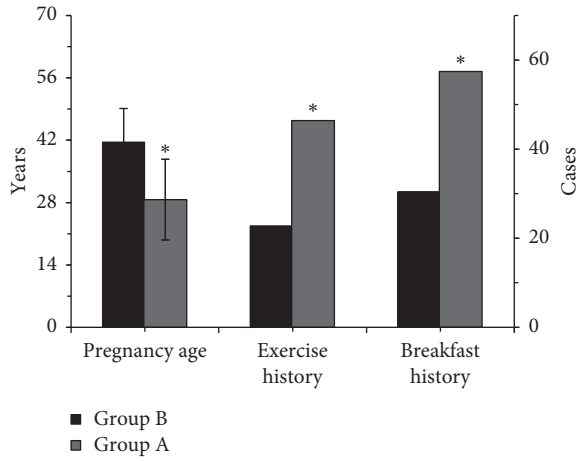

Figure 3: Comparison of the pregnancy age, exercise history, and breakfast history of pregnant women in the two groups. *Note*. *indicates that there was a statistically substantial difference in contrast to the algorithm of group B, $P < 0.05$.

women in group B with a history of exercise and breakfast was sharply less than that of group A, with a statistically great difference ($P < 0.05$).

Figure 4 reveals the comparison of BMI of pregnant women in the two groups. It indicates that the number of pregnant women in group B with BMI less than 25 kg/m^2 was hugely greater than that of group A, with a statistically marked difference ($P < 0.05$) while the number of pregnant women in group B with BMI greater than or equaled to 25 kg/m^2 was steeply less than that of group A, and the difference was statistically obvious ($P < 0.05$).

3.3. Color Doppler Ultrasound Images of Some Fetuses in the Pregnant Women with Gestational Diabetes Mellitus. The CDU image of the fetus of one pregnant woman from group B is shown in Figure 5; she was 36 years old. It revealed that the kidneys were clearly displayed without obvious abnormalities, and clear structures at the midline of the brain could be observed. These acoustic windows included the frontal suture, anterior fontanelle, and sagittal suture from front to back. The corpus callosum was slender and anechoic, and its upper and lower boundaries presented the linear high echo. Figure 6 indicates a case of CDU images of the fetus of one pregnant woman from group A (aged 25 years). It shows that there was no obvious abnormality in the structure of the kidneys. The ultrasound appearance of the pregnancy sac displayed a dark area in the center and a complete and uniformly thick echo around the dark area.

3.4. Comparison of Hemodynamic Parameters of Pulmonary Vein among Pregnant Women in the Two Groups. Figures 7 and 8 reveal the comparison results of S, D, S/D, A, and Tei index of the pulmonary veins of pregnant women in the two groups. It was found that the S/D and Tei index levels of pregnant women in group B were markedly increased by comparing with group A, with a statistically obvious difference ($P < 0.05$); the A level of pregnant women in group B were sharply lower than the level of group A, and the difference was statistically substantial ($P < 0.05$). In addition, the difference between the S and D levels of pregnant women in groups A and B was not statistically remarkable ($P > 0.05$).

3.5. Comparison of the Renal Artery Hemodynamic Parameters among Pregnant Women in the Two Groups. The comparison results of PI and RI among pregnant women in the two groups are reflected in Figure 9. PI of pregnant women in group B was 0.95 ± 0.15 and its RI was 1.94 ± 0.31, while PI and RI of pregnant women in group A were 0.57 ± 0.24 and 1.31 ± 0.27 in turn. Thus, PI and RI of pregnant women in group B were dramatically greater than those of group A, showing a statistically great difference ($P < 0.05$).

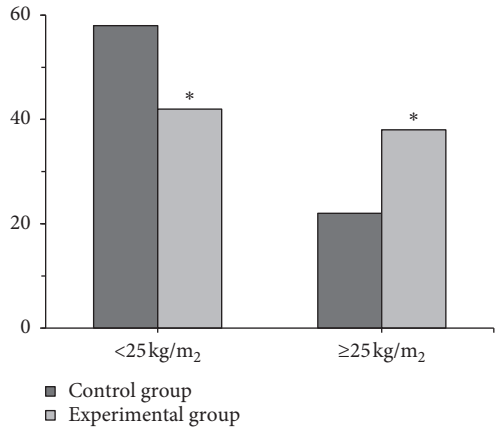

Figure 4: Comparison of BMI of pregnant women in the two groups. *Note*. * means that there was a statistically obvious difference was in contrast to the algorithm of group B ($P < 0.05$).

Figure 5: The CDU image of the fetus of one pregnant woman (aged 36 years) in group B.

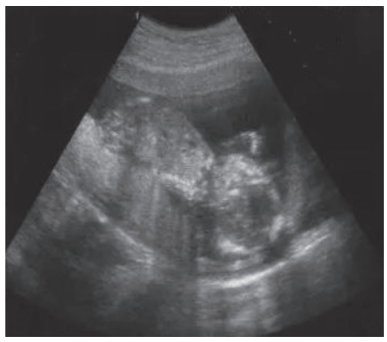

Figure 6: The CDU image of the fetus of one pregnant woman (aged 25 years) in group A.

3.6. Comparison of Gestational Age and Birth Weight of Fetuses in the Two Groups. There was a comparison of the gestational age and birth weight of fetuses in the two groups, as shown in Figure 10. It reveals that the gestational age of fetuses in group B was 34.17 ± 3.88 weeks, and the birth weight of fetuses was 4.114 ± 0.547 kg. Moreover, the gestational age and birth weight of fetuses in group A were 38.66 ± 2.75 weeks and 3.281 ± 0.429 kg in sequence. The

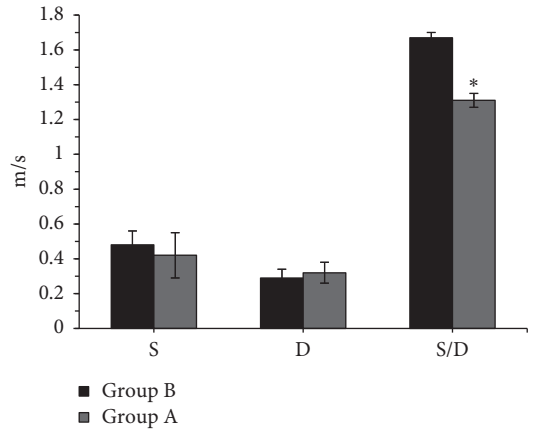

Figure 7: Comparison of S, D, and S/D of pulmonary veins among pregnant women in the two groups. *Note*. * indicates that the difference was statistically considerable compared to group B, $P < 0.05$.

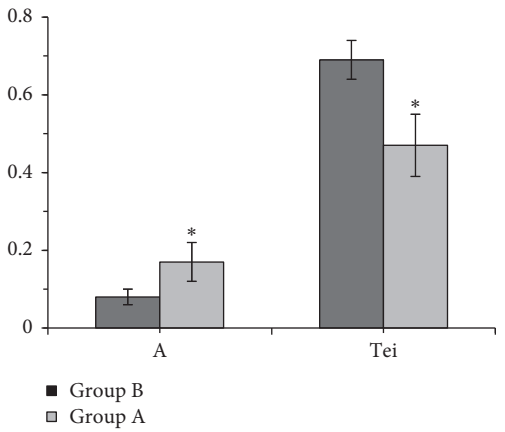

Figure 8: Comparison of A and Tei index levels of pulmonary veins among pregnant women in the two groups. *Note*. * indicates that the difference was statistically considerable in contrast to group B, $P < 0.05$.

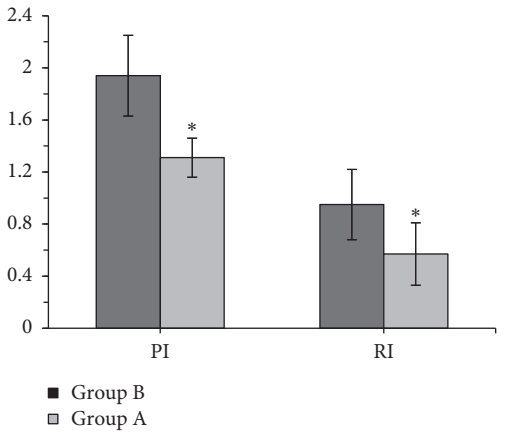

Figure 9: Comparison of PI and RI of pregnant women in groups A and B. *Note*. * reveals that the difference was statistically great in contrast to group B, $P < 0.05$.

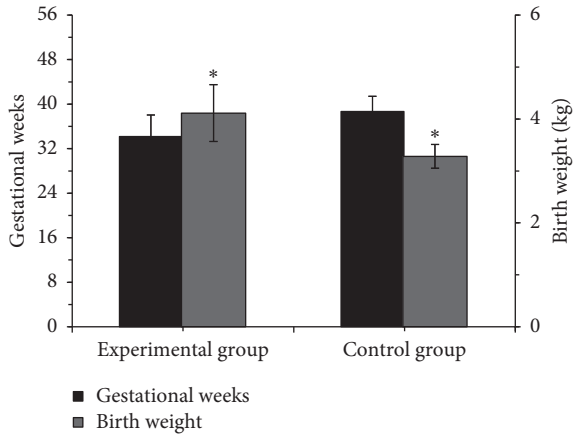

Figure 10: Comparison of gestational age and birth weight of fetuses in the two groups. *Note*. *indicates a notable difference in gestational age versus the experimental group, $P < 0.05$, and #indicates a notable difference in birth weight versus the experimental group, $P < 0.05$.

gestational age of fetuses in group B was greatly shorter than that of group A ($P < 0.05$).

3.7. Regression Analysis of Factors Related to Gestational Diabetes Mellitus in Pregnant Women. As shown in Table 1, the dependent variable was whether a pregnant woman suffered from DM (1 for the pregnant woman with DM and 0 for the pregnant woman without DM), and pregnancy age, BMI, exercise history, breakfast history, anemia, family history of hypertension, and abortion history were regarded as independent variables for single-factor regression analysis. It suggested that pregnancy age, BMI, family history of hypertension, and abortion history were all extremely positively correlated with GDM in pregnant women ($P < 0.05$), and exercise history and breakfast history were all greatly negatively related with GDM in pregnant women ($P < 0.05$). What is more, there was a marked negative correlation between anemia and GDM in pregnant women ($P < 0.05$).

The dependent variable was whether a pregnant woman had DM (pregnant woman with DM was for 1 and pregnant woman without DM was for 0), and multiple factors regression analysis was used for the independent variables (pregnancy age, BMI, exercise history, breakfast history, family history of hypertension, and abortion history) (Table 2). There was a substantially positive correlation of pregnancy age, family history of hypertension, and abortion history with GDM in pregnant women ($P < 0.05$). However, BMI, exercise history, and breakfast history were not extremely related to GDM in pregnant women ($P > 0.05$).

4. Discussion

GDM refers to abnormal glucose metabolism that occurs during pregnancy, with an incidence rate of 1%–5%. When DM occurs, insufficient insulin secretion will cause a series of metabolic disorders such as glucose, protein, fat, water, and electrolytes. As a stress factor, pregnancy can aggravate various metabolic disorders and even ketoacidosis or hyperosmolar nonketosis diabetes coma [15]. The clinical process of GDM is more complicated, and the maternal and infant mortality rate is still high. If not treated in time, it can lead to abortion, premature delivery, stillbirth, polyhydramnios, giant fetus, and fetal malformation. Therefore, it is very critical to monitor the change of pregnant women's signs in time [16]. In this study, BPC was compared with the introduced APES and LCA, respectively. The results revealed that the Dice similarity coefficient, sensitivity, and specificity of BPC were markedly greater than those of APES and LCA, but its running time was extremely shorter than that of APES and LCA ($P < 0.05$), which indicated that the BPC constructed in this study had an excellent performance in the diagnosis of infant CDU images. It could not only promote the diagnosis accuracy but also reduce the running time [17].

The pregnancy age of pregnant women in group B was considerably greater than that of group A, and the number of pregnant women with exercise history and breakfast history dropped obviously in contrast to group A ($P < 0.05$). This was similar to the research results of Thapa et al. [18]. Every organ function, insulin receptor, and insulin affinity decreased with the growth of pregnancy age, indicating that pregnancy age, regular exercise, and regular breakfast might have an impact on pregnant women with GDM [19]. The S/D and Tei index of pregnant women in group B were obviously higher than those of group A, and the level of A was sharply lower than the level of group A ($P < 0.05$), showing that pregnant women with high blood glucose would affect

Table 1: Single-factor regression analysis of related factors of GDM in pregnant women.

Variable	Regression coefficient	t	P
Pregnancy age	0.426	4.721	0.011*
BMI	0.399	3.865	0.008*
Exercise history	−0.421	3.477	0.037#
Breakfast history	−0.415	4.156	0.019#
Anemia	−0.215	2.831	0.051
Family history of hypertension	0.361	3.864	0.007*
Abortion history	0.407	4.666	0.016*

Note. *indicates obvious positive correlation with GDM, $P < 0.05$; #indicates obvious negative correlation with GDM, $P < 0.05$.

Table 2: Multivariate regression analysis of related factors of GDM in pregnant women.

Variable	Regression coefficient	t	P
Pregnancy age	0.326	3.755	0.032*
BMI	0.207	1.875	0.065
Exercise history	0.221	2.677	0.052
Breakfast history	0.160	2.236	0.059
Family history of hypertension	0.389	3.694	0.014*
Abortion history	0.445	4.237	0.024*

Note. *indicates obvious positive correlation with GDM, $P < 0.05$.

the heart function of the fetuses. The PI and RI of pregnant women in group B increased markedly compared with group A ($P < 0.05$), which was consistent with the research findings of Duan et al. [20]. It suggested that the ultrasound examination of the fetal pulmonary vein and renal artery blood could reflect the fetal hypoxia in the uterus. Multivariate regression analysis revealed that pregnancy age, family history of hypertension, and abortion history were markedly positively associated with GDM in pregnant women ($P < 0.05$), which showed that pregnancy age, family history of hypertension, and abortion history were the related risk factors for GDM in pregnant women.

5. Conclusion

The constructed BPC in this study was compared with APES and LCA and applied to the CDU imaging diagnosis of 80 pregnant women with GDM. It was found that the BPC had excellent performance in infant CRU imaging diagnosis, which not only enhanced the diagnosis accuracy but also decreased the calculation time. Age of pregnancy, family history of hypertension, and abortion history were the related risk factors leading to GDM in pregnant women. However, the number of pregnant women selected in this study is small, and the follow-up time is relatively short, which would reduce the power of the study and increase the margin of error. In the future, the sample size should be increased to further explore the risk factors of GDM. The study innovatively analyzed the correlation between pregnancy weight and birth weight with the GDM and the results provided a good theoretical basis for the clinical diagnosis and treatment of GDM.

Data Availability

No data were used to support this study.

Conflicts of Interest

None of the authors have any conflicts of interest.

References

[1] C. Schneeberger, J. J. H. M. Erwich, E. R. V. D. Heuvel, B. W. J. Mol, A. Ott, and S. E. Geerlings, "Asymptomatic bacteriuria and urinary tract infection in pregnant women with and without diabetes: cohort study," *and Gynecology and Reproductive Biology*, vol. 222, pp. 176–181, 2018.

[2] A. L. F. Gomez, H. L. Barrett, and H. D. McIntyre, "Increased systolic and diastolic blood pressure is associated with altered gut microbiota composition and butyrate production in early pregnancy," *Hypertension*, vol. 68, no. 4, pp. 974–981, 2016.

[3] P. Dervisoglu, M. Kosecik, and S. Kumbasar, "Effects of gestational and pregestational diabetes mellitus on the foetal heart: a cross-sectional study," *Journal of Obstetrics and Gynaecology*, vol. 38, no. 3, pp. 408–412, 2018.

[4] R. H. A. Rifai and F. Aziz, "Prevalence of type 2 diabetes, prediabetes, and gestational diabetes mellitus in women of childbearing age in Middle East and North Africa, 2000-2017: protocol for two systematic reviews and meta-analyses," *Systematic Reviews*, vol. 7, no. 1, p. 96, 2018.

[5] A. Soliman, H. Salama, and R. H. A. Rifai, "The effect of different forms of dysglycemia during pregnancy on maternal and fetal outcomes in treated women and comparison with large cohort studies," *Acta Bio-Medica: Atenei Parmensis*, vol. 89, no. S5, pp. 11–21, 2018.

[6] P. B. Renz, M. K. Hernandez, and J. L. Camargo, "Effect of iron supplementation on HbA1c levels in pregnant women with and without anaemia," *Clinica Chimica Acta*, vol. 478, pp. 57–61, 2018.

[7] B. C. Benfica, T. Zanella, L. Farias, M. Oppermann, L. Canani, and D. Lavinsky, "Macular choroidal thickness in pregnant women with type 1, type 2 and gestational diabetes mellitus measured by spectral-domain optical coherence tomography," *Clinical Ophthalmology*, pp. 1259–1265, 2018.

[8] J. E. Dominguez, A. S. Habib, and A. D. Krystal, "A review of the associations between obstructive sleep apnea and hypertensive disorders of pregnancy and possible mechanisms of disease," *Sleep Medicine Reviews*, vol. 42, pp. 37–46, 2018.

[9] B. Altıparmak, N. Çelebi, Ö Canbay, M. K Toker, B Kılıçarslan, and Ü Aypar, "Effect of magnesium sulfate on anesthesia depth, awareness incidence, and postoperative pain scores in obstetric patients. A double-blind randomized controlled trial," *Saudi Medical Journal*, vol. 39, no. 6, pp. 579–585, 2018.

[10] D. S. L. B. Gabriel, E. L. Rosado, D. P. Carvalho et al., "Food intake of women with gestational diabetes mellitus, in accordance with two methods of dietary guidance: a randomised controlled clinical trial," *British Journal of Nutrition*, vol. 121, no. 1, pp. 82–92, 2019.

[11] C. Hamel, E. Lang, K. Morissette et al., "Screening for depression in women during pregnancy or the first year postpartum and in the general adult population: a protocol for two systematic reviews to update a guideline of the Canadian Task Force on Preventive Health Care," *Systematic Reviews*, vol. 8, no. 1, 2019.

[12] M. Deghatipour, Z. Ghorbani, S. Ghanbari et al., "Oral health status in relation to socioeconomic and behavioral factors among pregnant women: a community-based cross-sectional study," *BMC Oral Health*, vol. 19, no. 1, 2019.

[13] S. T. Schütze, T. Groten, E. Schleussner, and W. Battefeld, "Evaluation of treatment strategies to manage diabetes mellitus in pregnancy: use of fetal sonography compared to monitoring of maternal blood glucose alone," *Geburtshilfe und Frauenheilkunde*, vol. 79, no. 11, pp. 1199–1207, 2019.

[14] N. M. Nielsen, K. L. Munger, H. N. Koch et al., "Neonatal vitamin D status and risk of multiple sclerosis," *Neurology*, vol. 88, no. 1, pp. 44–51, 2017.

[15] C. S. Nelson, C. D. Vera, and M Su, "Intrahost dynamics of human cytomegalovirus variants acquired by seronegative glycoprotein B vaccinees," *Journal of Virology*, vol. 93, no. 5, Article ID e01695, 2019.

[16] K. Wongdee, N. Krishnamra, and N. Charoenphandhu, "Derangement of calcium metabolism in diabetes mellitus: negative outcome from the synergy between impaired bone turnover and intestinal calcium absorption," *The Journal of Physiological Sciences*, vol. 67, no. 1, pp. 71–81, 2017.

[17] R. H. Gurbuz, P. Atilla, G. Orgul et al., "Impaired placentation and early pregnancy loss in patients with MTHFR polymorphisms and type-1 diabetes mellitus," *Fetal and Pediatric Pathology*, vol. 38, no. 5, pp. 376–386, 2019.

[18] P. Thapa, A. H. Bangura, I. Nirola et al., "The power of peers: an effectiveness evaluation of a cluster-controlled trial of group antenatal care in rural Nepal," *Reproductive Health*, vol. 16, no. 1, 2019.

[19] J. F. Melo, V. N. J. Bravo, L. M. M. Nardozza et al., "Reference range of fetal myocardial area by three-dimensional ultrasonography and its applicability in fetuses of pre-gestational diabetic women," *Journal of Perinatal Medicine*, vol. 47, no. 4, pp. 422–428, 2019.

[20] Y. Duan, F. Sun, S. Que, Y Li, S Yang, and G Liu, "Pre-pregnancy maternal diabetes combined with obesity impairs placental mitochondrial function involving Nrf2/ARE pathway and detrimentally alters metabolism of offspring," *Obesity Research and Clinical Practice*, vol. 12, no. 2, pp. 90–100, 2018.